Figure S1

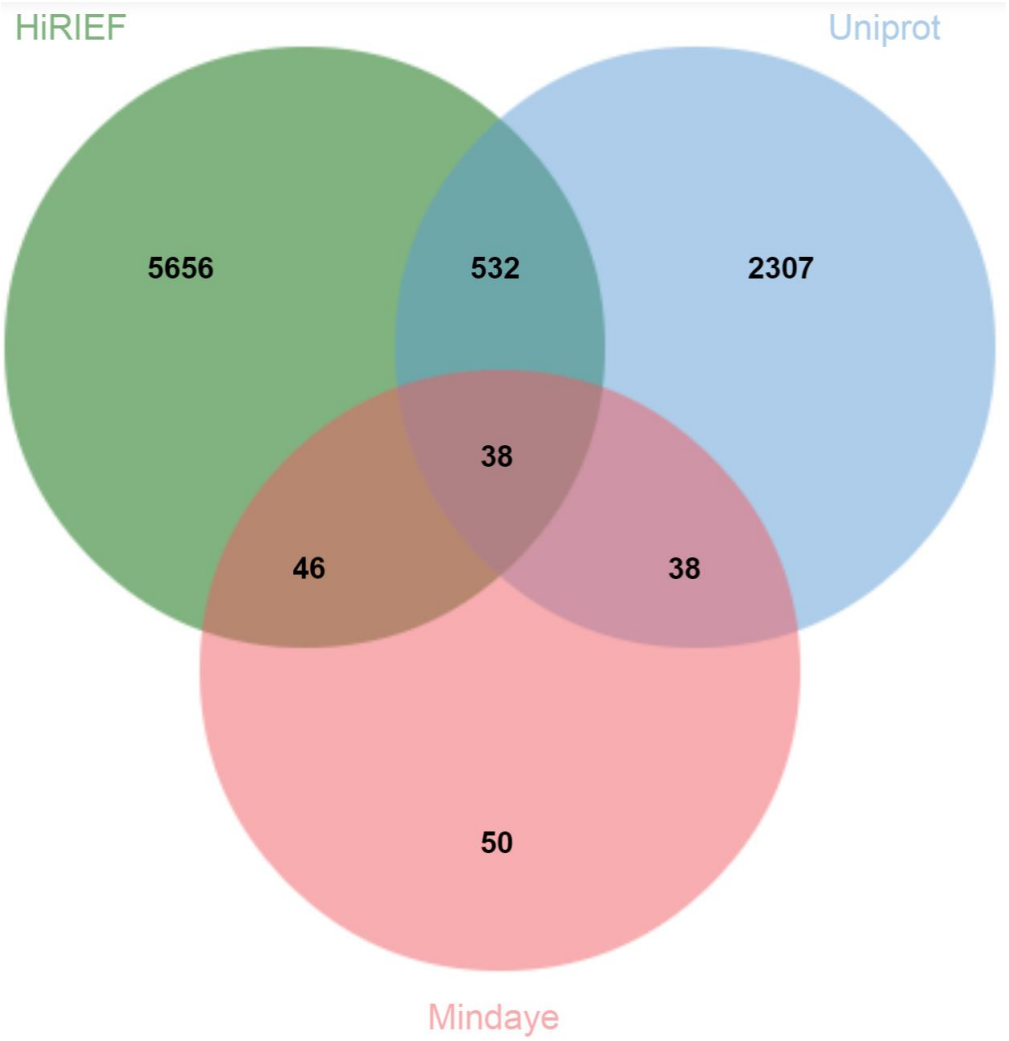

Figure S1 Detection of MSC membrane associated proteins. Venn diagram showing overlap of detected membrane associated proteins between our consensus cellular MSC HiRIEF LC-MS/MS data (detected in all 9 samples) and the consensus Mindaye *et al* MSC proteome dataset (detected in all 4 samples) and the Uniprot human proteome database.

Figure S2

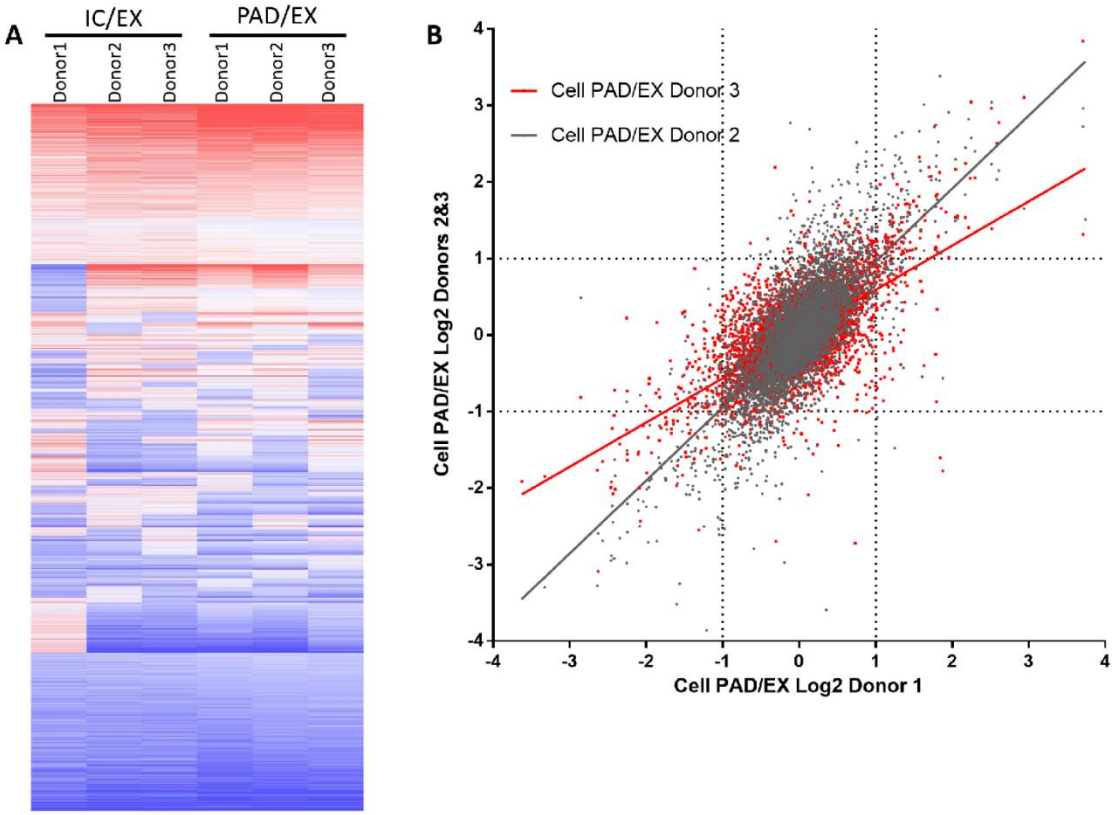

Figure S2 Representative concordance and variation between MSC donors. (A) Heatmap of cellular global proteome expression differentials between IC/EX and PAD/EX across all 3 donors reveals some donor to donor variation as well as intra-condition and intra-donor concordance. **(B)** Comparison of PAD/EX donor ratios from all 3 donors reveals some donor to donor variation as well as intra-condition and intra-donor concordance. Red dots represent PAD/EX protein expression ratios of donor 3 vs donor 1. Red line represents regression analysis of PAD/EX protein expression ratios of donor 3 vs donor 1. Grey dots represent PAD/EX protein expression ratios of donor 2 vs donor 1. Grey line represents regression analysis of PAD/EX protein expression ratios of donor 2 vs donor 1.

Figure S3

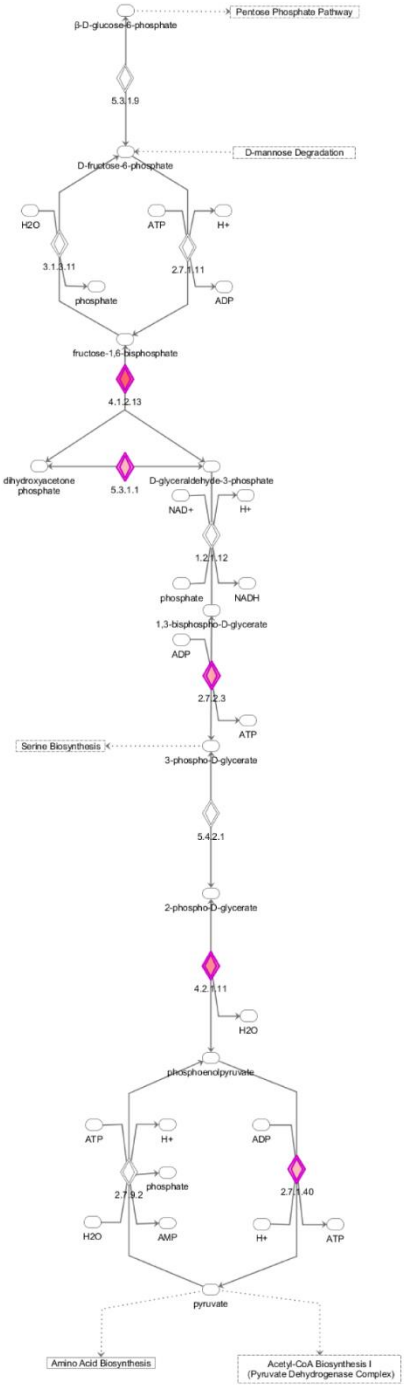

Figure S3 Upregulation of glycolysis pathway proteins in PAD/EX. Ingenuity Pathway Analysis of differentially expressed cellular proteins (FDR-1%) revealed increased expression of key regulators of glycolysis in the PAD condition as compared to the EX condition. Red boxes indicate increased expression, green boxes indicate decreased expression and white boxes indicate no significant change in expression or presence not detected. Analysis of 3 different donors per condition. For differential expression T-tests with multiple testing correction with an FDR of 1% was used.

Figure S4

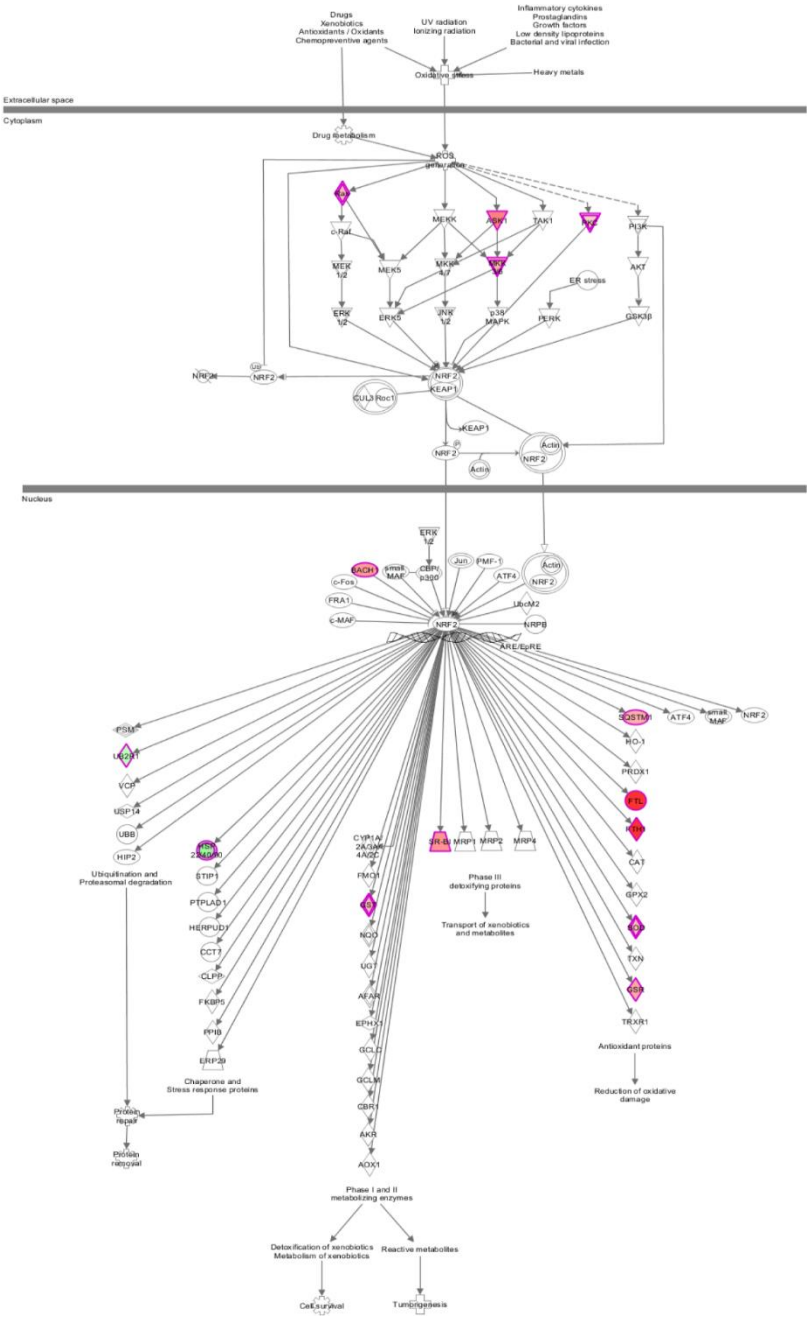

Figure S4 Upregulation of NRF2 pathway proteins in PAD/EX. Ingenuity Pathway Analysis of differentially expressed cellular proteins (FDR-1%) revealed increased expression of key regulators of the NRF2 pathway, which is the master regulator of glutathione synthesis, in the PAD condition as compared to the EX condition. Red boxes indicate increased expression, green boxes indicate decreased expression and white boxes indicate no significant change in expression or presence not detected. Analysis of 3 different donors per condition. For differential expression T-tests with multiple testing correction with an FDR of 1% was used.

Figure S5

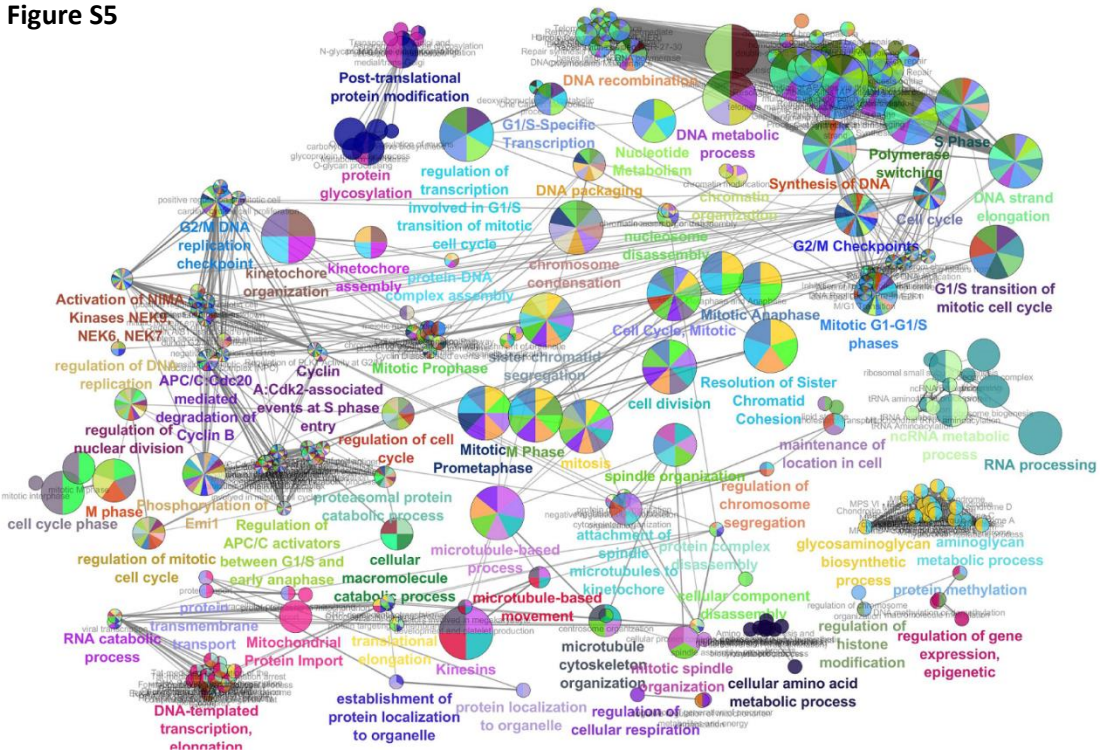

Figure S5 Downregulation of proliferation and cell cycle checkpoint associated pathways in PAD/EX. Functional Gene Ontology analysis (CytoScape/ClueGO) of all significantly downregulated cellular proteins (FDR-1%) revealed decreased expression of key regulators cellular proliferation and cell cycle checkpoint related pathways. Analysis of 3 different donors per condition. For differential expression T-tests with multiple testing correction with an FDR of 1% was used. Circles are color coded according to their associated functionality. Number of circles and larger diameter of circles indicate greater over representation.

Figure S6

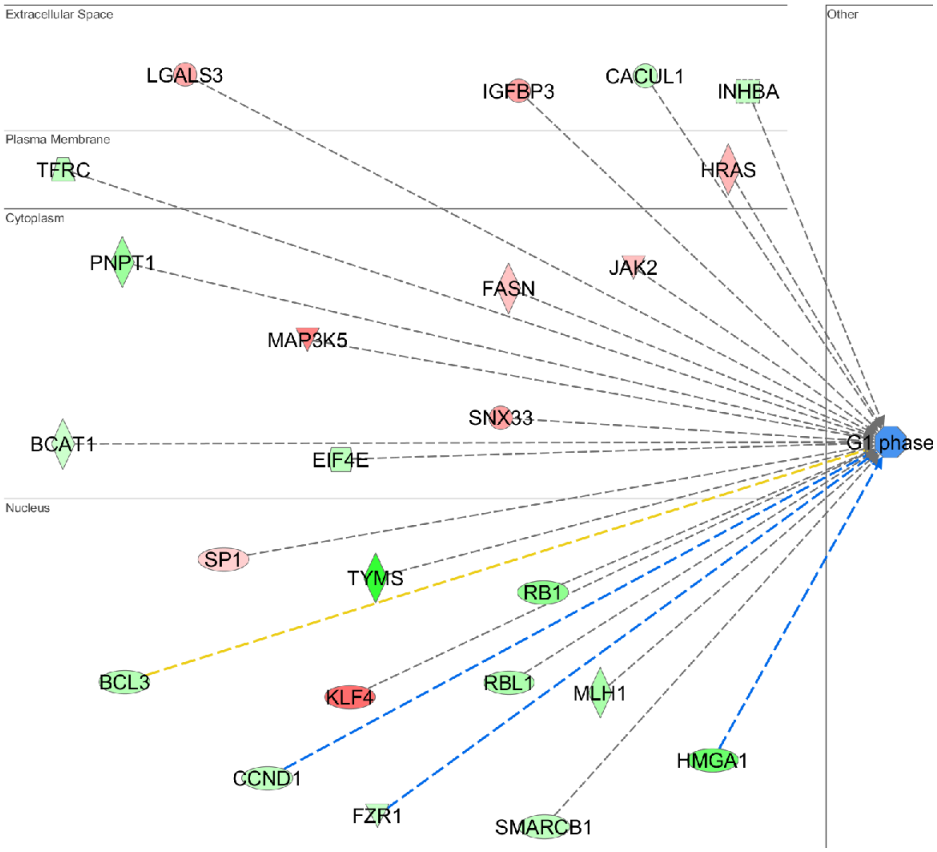

Figure S6 Predicted inhibition of G1 phase progression in PAD/EX. Ingenuity Pathway Analysis of differentially expressed cellular proteins (FDR-1%) revealed down regulation of G1 phase proteins in the PAD condition as compared to the EX condition. Red boxes indicate increased expression, green boxes indicate decreased expression. Orange lines indicate predicted increased target functionality, blue lines indicate predicted decreased target functionality, grey lines are undetermined and yellow lines are inconsistent. Horizontal lines represent canonical subcellular localization of protein. Analysis of 3 different donors per condition. For differential expression T-tests with multiple testing correction with an FDR of 1% was used.

Figure S7

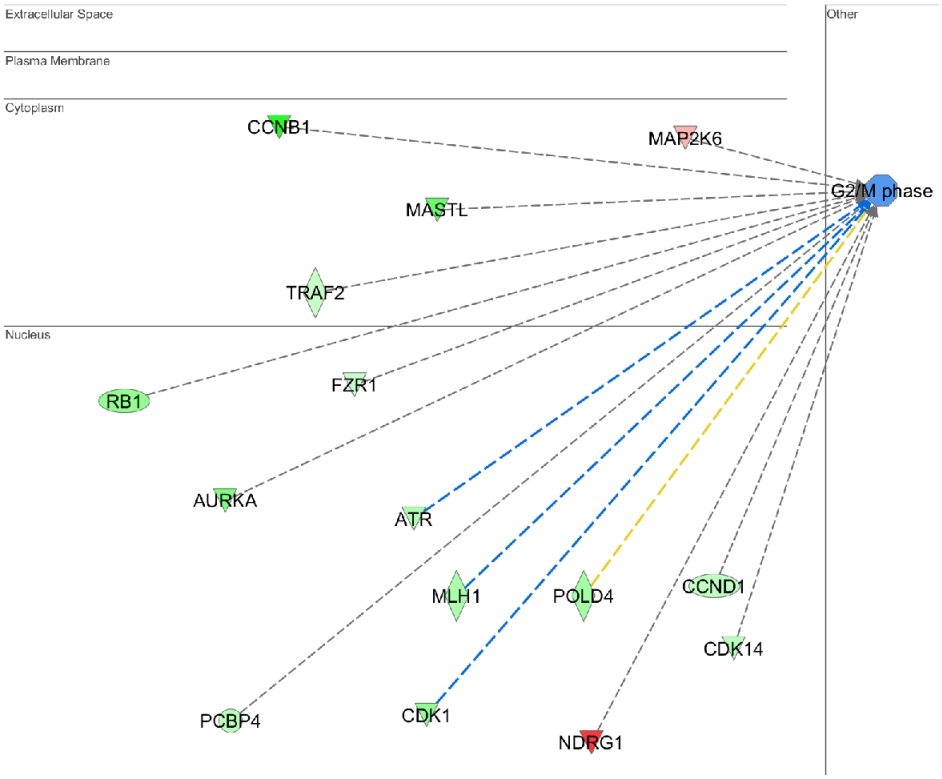

Figure S7 Predicted inhibition of G2/M phase progression in PAD/EX. Ingenuity Pathway Analysis of differentially expressed cellular proteins (FDR-1%) revealed down regulation of G2/M phase proteins in the PAD condition as compared to the EX condition. Red boxes indicate increased expression, green boxes indicate decreased expression. Orange lines indicate predicted increased target functionality, blue lines indicate predicted decreased target functionality, grey lines are undetermined and yellow lines are inconsistent. Horizontal lines represent canonical subcellular localization of protein. Analysis of 3 different donors per condition. For differential expression T-tests with multiple testing correction with an FDR of 1% was used.

Figure S8

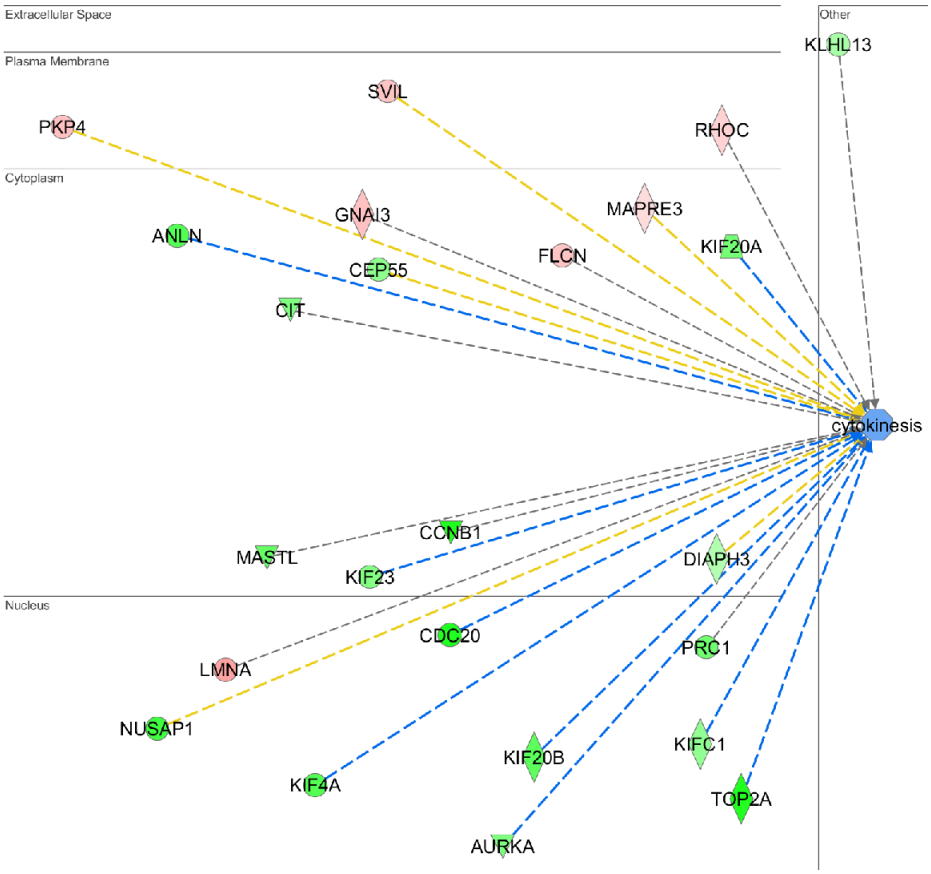

Figure S8 Predicted inhibition of cytokinesis in PAD/EX. Ingenuity Pathway Analysis of differentially expressed cellular proteins (FDR-1%) revealed down regulation of cytokinesis associated proteins in the PAD condition as compared to the EX condition. Red boxes indicate increased expression, green boxes indicate decreased expression. Orange lines indicate predicted increased target functionality, blue lines indicate predicted decreased target functionality, grey lines are undetermined and yellow lines are inconsistent. Horizontal lines represent canonical subcellular localization of protein. Analysis of 3 different donors per condition. For differential expression T-tests with multiple testing correction with an FDR of 1% was used.

Figure S9

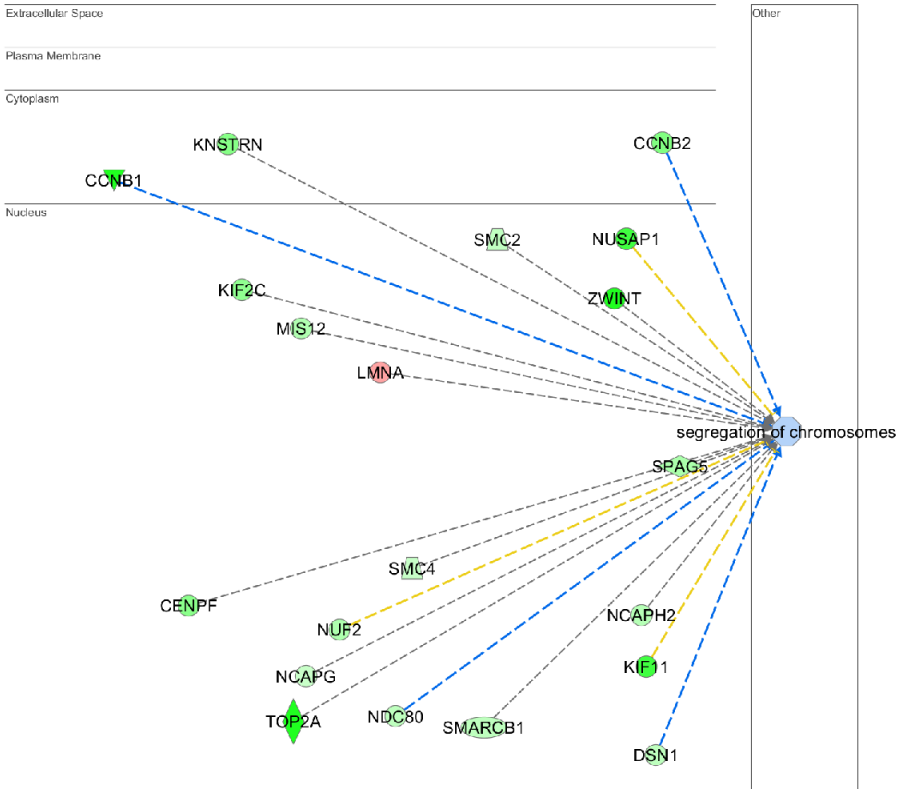

Figure S9 Predicted inhibition of chromosomal segregation in PAD/EX. Ingenuity Pathway Analysis of differentially expressed cellular proteins (FDR-1%) revealed down regulation of proteins associated with segregation of chromosomes in the PAD condition as compared to the EX condition. Red boxes indicate increased expression, green boxes indicate decreased expression. Orange lines indicate predicted increased target functionality, blue lines indicate predicted decreased target functionality, grey lines are undetermined and yellow lines are inconsistent. Horizontal lines represent canonical subcellular localization of protein. Analysis of 3 different donors per condition. For differential expression T-tests with multiple testing correction with an FDR of 1% was used.

Figure S10

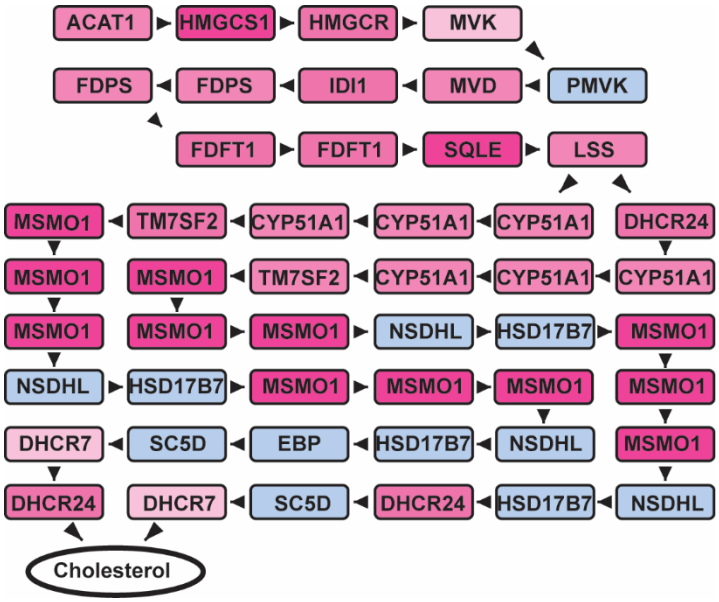

Figure S10 Upregulation of cholesterol biosynthesis pathway proteins in PAD/EX. Ingenuity Pathway Analysis of differentially expressed cellular proteins (FDR-1%) revealed upregulation of proteins associated with the cholesterol biosynthesis pathway in the PAD condition as compared to the EX condition. Red boxes indicate increased expression, blue boxes indicate lack of detection. Analysis of 3 different donors per condition. For differential expression T-tests with multiple testing correction with an FDR of 1% was used.

Figure S11

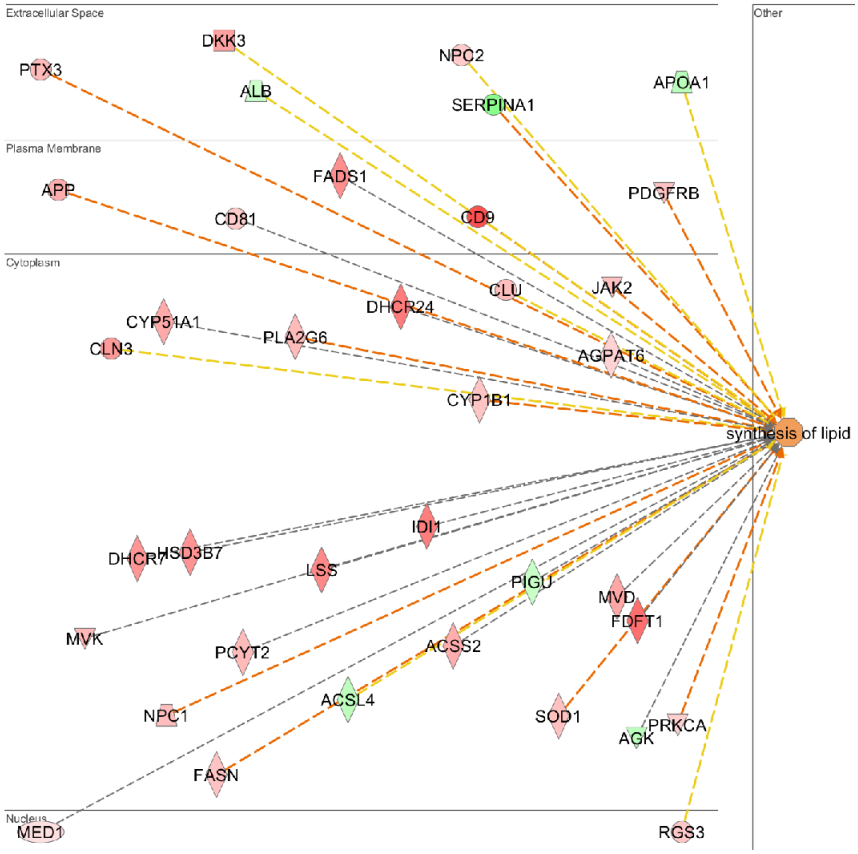

Figure S11 Predicted induction of lipid biosynthesis in PAD/EX. Ingenuity Pathway Analysis of differentially expressed cellular proteins (FDR-1%) revealed down regulation of proteins associated with lipid biosynthesis in the PAD condition as compared to the EX condition. Red boxes indicate increased expression, green boxes indicate decreased expression. Orange lines indicate predicted increased target functionality, blue lines indicate predicted decreased target functionality, grey lines are undetermined and yellow lines are inconsistent. Horizontal lines represent canonical subcellular localization of protein. Analysis of 3 different donors per condition. For differential expression T-tests with multiple testing correction with an FDR of 1% was used.

Figure S12

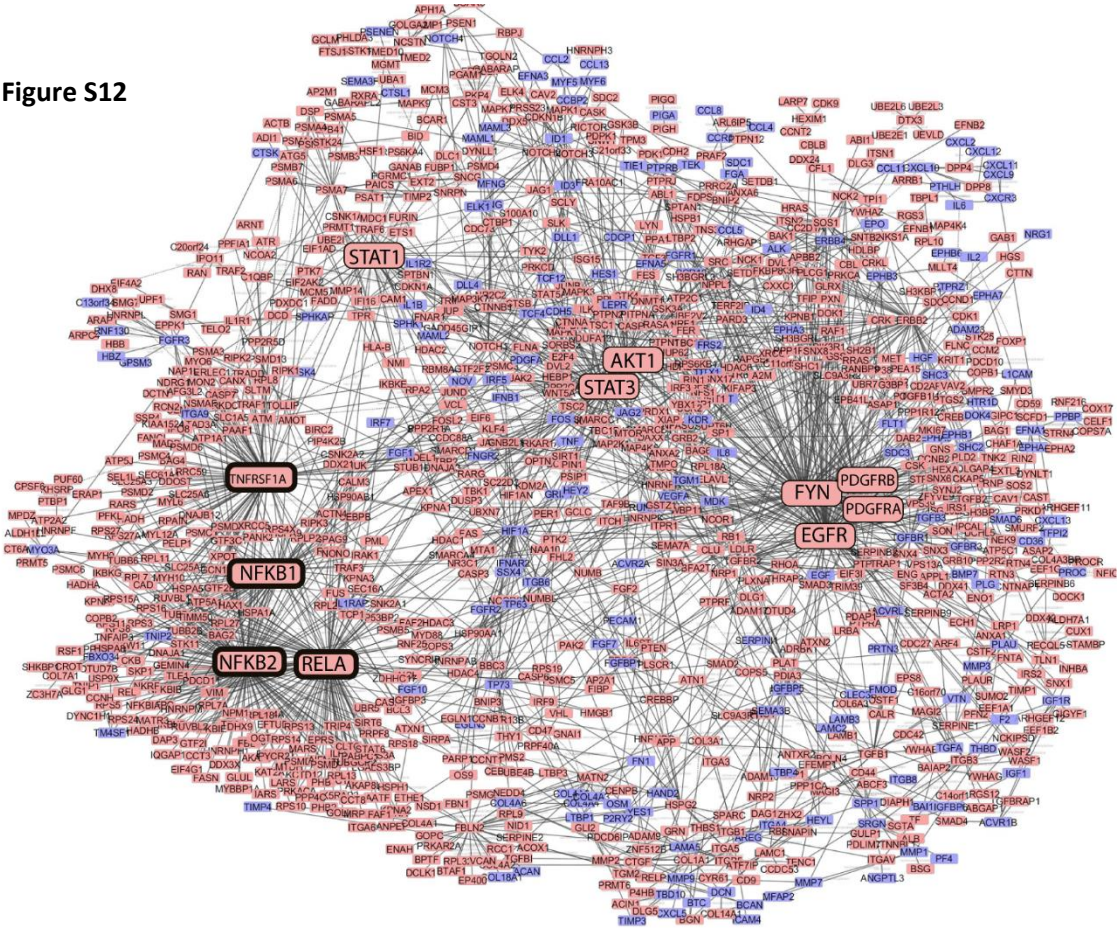

Figure S12 MSC angiogenesis interactome network analysis. Network analysis of the MSC angiogenesis interactome reveals the most robust clustering around nodes involved in NFkB signaling (embolden boxes). Analysis performed using CytoScape. Red boxes indicates presence in angiome interacting proteins in MSCs, blue boxes indicate absence of these proteins in MSCs. Boxes of major clustering nodes of known effectors were enlarged for clarity. Edges connecting boxes indicates experimental evidence of physical contact (eg co-immunopreciptitation, yeast-2-hybrid).

Figure S13

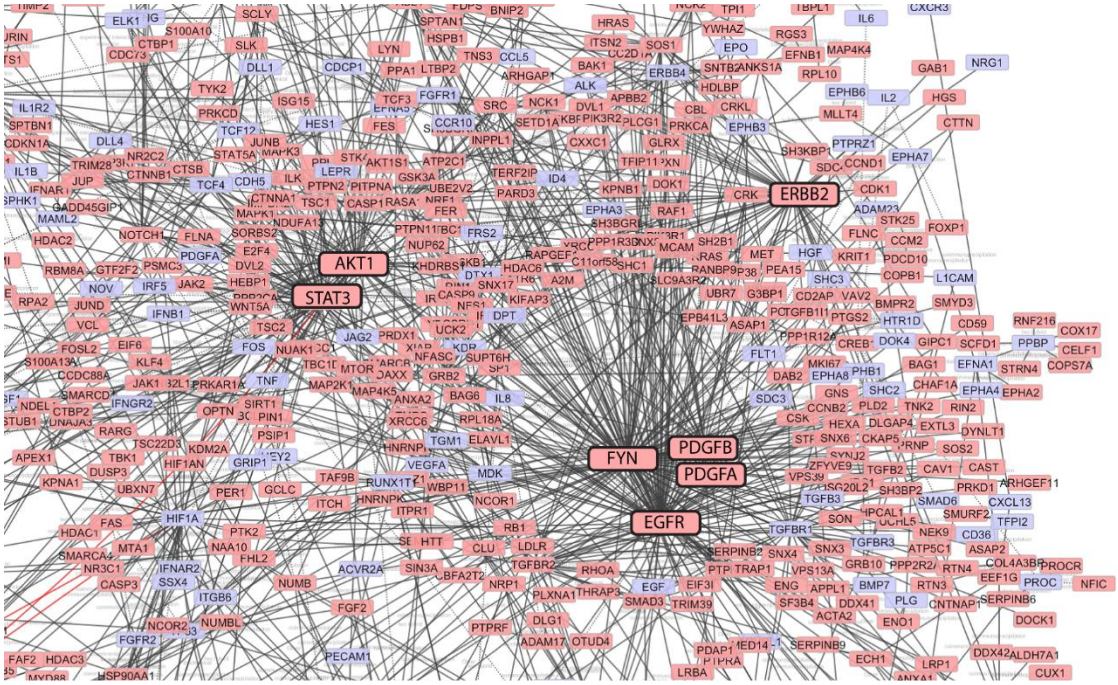

Figure S13 MSC angiogenesis interactome network analysis. Zoomed in view of network analysis of the MSC angiogenesis interactome reveals clustering around PDGFRA, PDGFRB and EGFR nodes. Analysis performed using CytoScape. Red boxes indicates presence in angiome interacting proteins in MSCs, blue boxes indicate absence of these proteins in MSCs. Boxes of major clustering nodes of known effectors were enlarged for clarity. Edges connecting boxes indicates experimental evidence of physical contact (eg co-immunopreciptitation, yeast-2-hybrid).

Figure S14

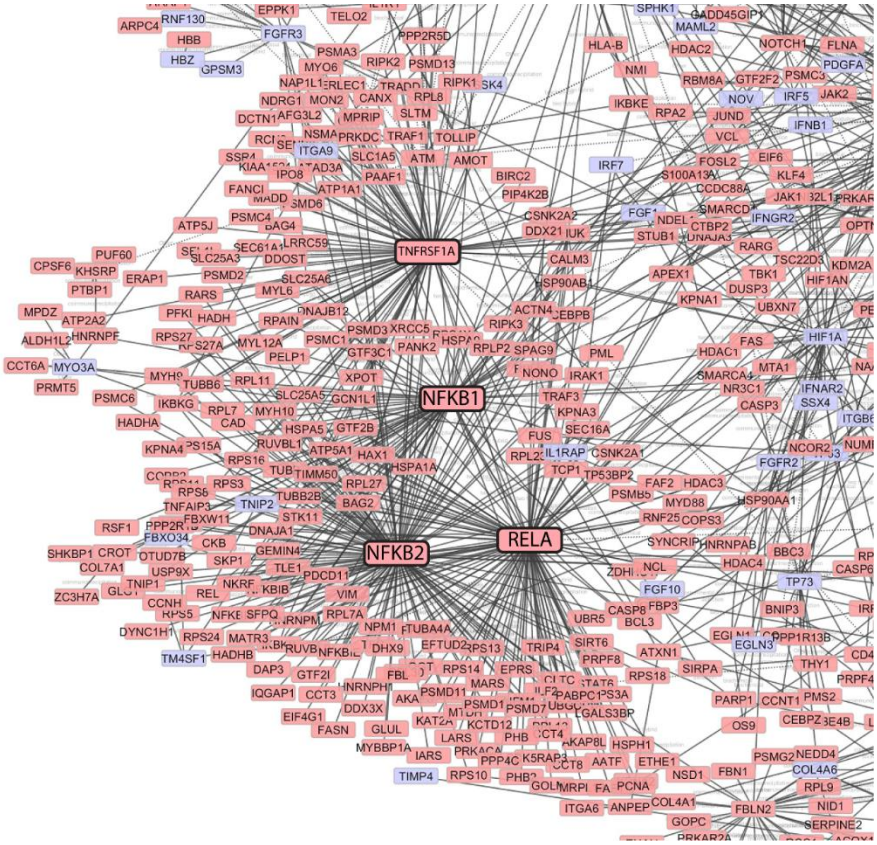

Figure S14 MSC angiogenesis interactome network analysis. Close up view of network analysis of the MSC angiogenesis interactome reveals the most robust clustering around NFkB1, NFkB2 and RELA nodes. Analysis performed using CytoScape. Red boxes indicates presence in angiome interacting proteins in MSCs, blue boxes indicate absence of these proteins in MSCs. Boxes of major clustering nodes of known effectors were enlarged for clarity. Edges connecting boxes indicates experimental evidence of physical contact (eg co-immunopreciptitation, yeast-2-hybrid).

Figure S15

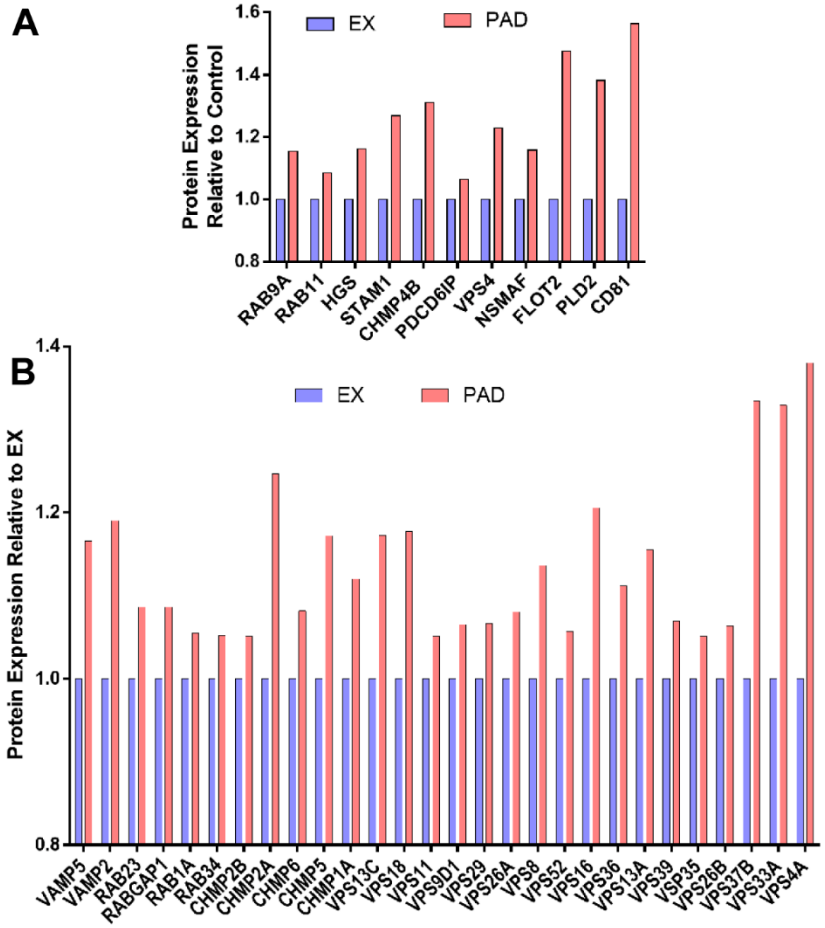

Figure S15 Upregulation of exosome biogenesis proteins in PAD/EX. (A) Relative expression of known exosome biogenesis proteins demonstrated a trend towards increased expression in PAD/EX. **(B)** Vesicle associated protein family members demonstrated a trend towards increased expression in PAD/EX.

Figure S16

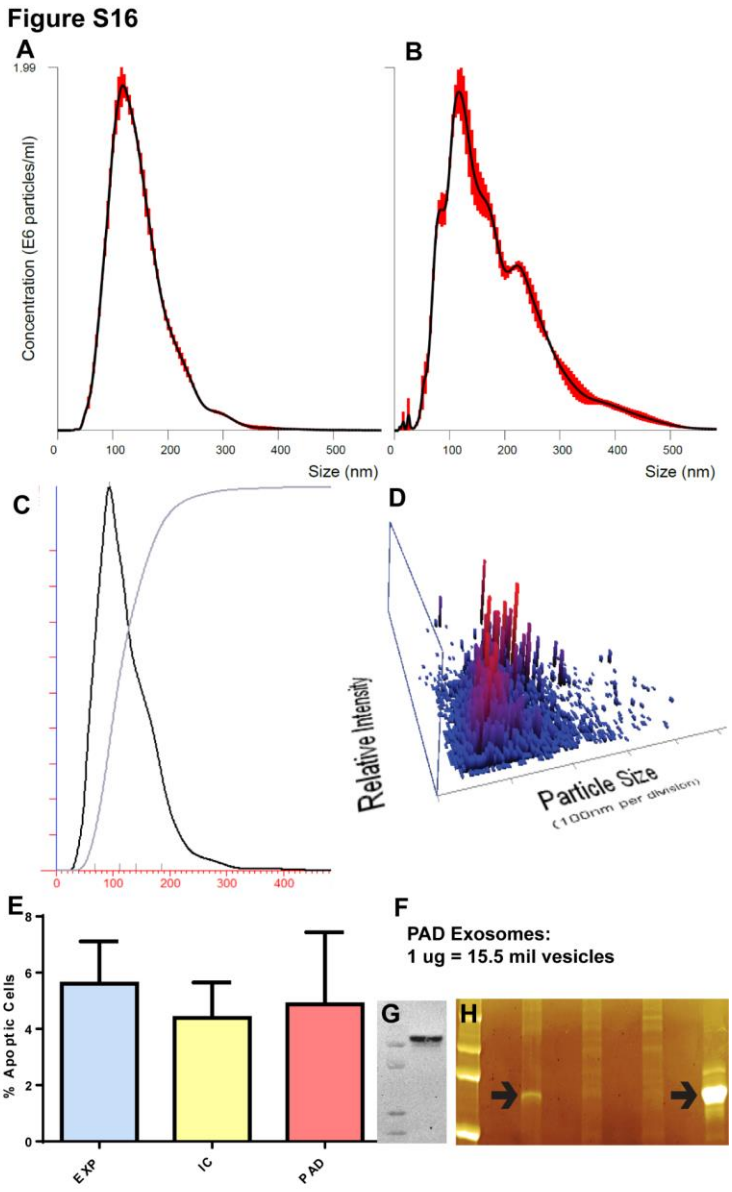

Figure S16 Size distribution analysis of MSC exosomes. (A-D) Nanosight tracking analysis showing the size distribution of MSC exosome and relative intensity for EX **(A)**, IC **(B)** and PAD **(C,D)**. **(E)** Low levels of apoptosis of MSCs from all 3 conditions (EX, IC and PAD), shows no significant differences between the conditions. **(F)** Conversion factor of MSC exosomes from PAD condition, number of vesicles per ug of exosomal protein. **(G)** Western blot analysis identified the presence of exosomal marker protein Alix in PAD exosomes. **(H)** Coomassie blue staining of protein demonstrate EX exosomes co-isolated with FBS protein of 65 kDa size (arrows), which is bovine serum albumin protein. First lane = molecular weight ladder, second lane = exosomes from EX, third lane = exosomes from IC, forth lane = fresh EX media (20% FBS).

Figure S17

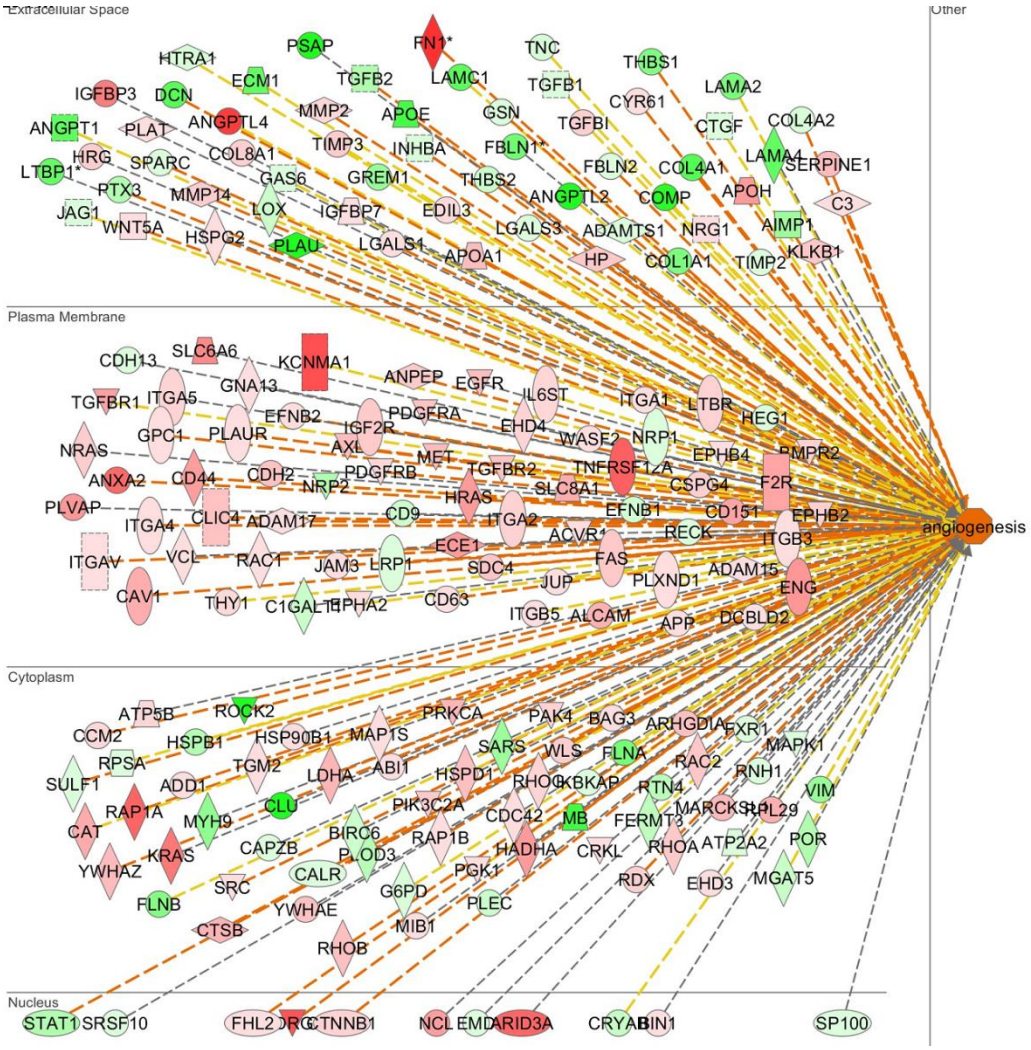

Figure S17 Predicted induction of angiogenesis by MSC exosomal protein content. Ingenuity Pathway Analysis of detected MSC exosome proteins (FDR-1%) revealed presence of proteins associated with angiogenesis potentiation. Red boxes indicate increased expression, green boxes indicate decreased expression. Orange lines indicate predicted increased target functionality, blue lines indicate predicted decreased target functionality, grey lines are undetermined and yellow lines are inconsistent. Horizontal lines represent canonical subcellular localization of protein. Analysis of 3 different donors per condition. For differential expression T-tests with multiple testing correction with an FDR of 1% was used.

Figure S18

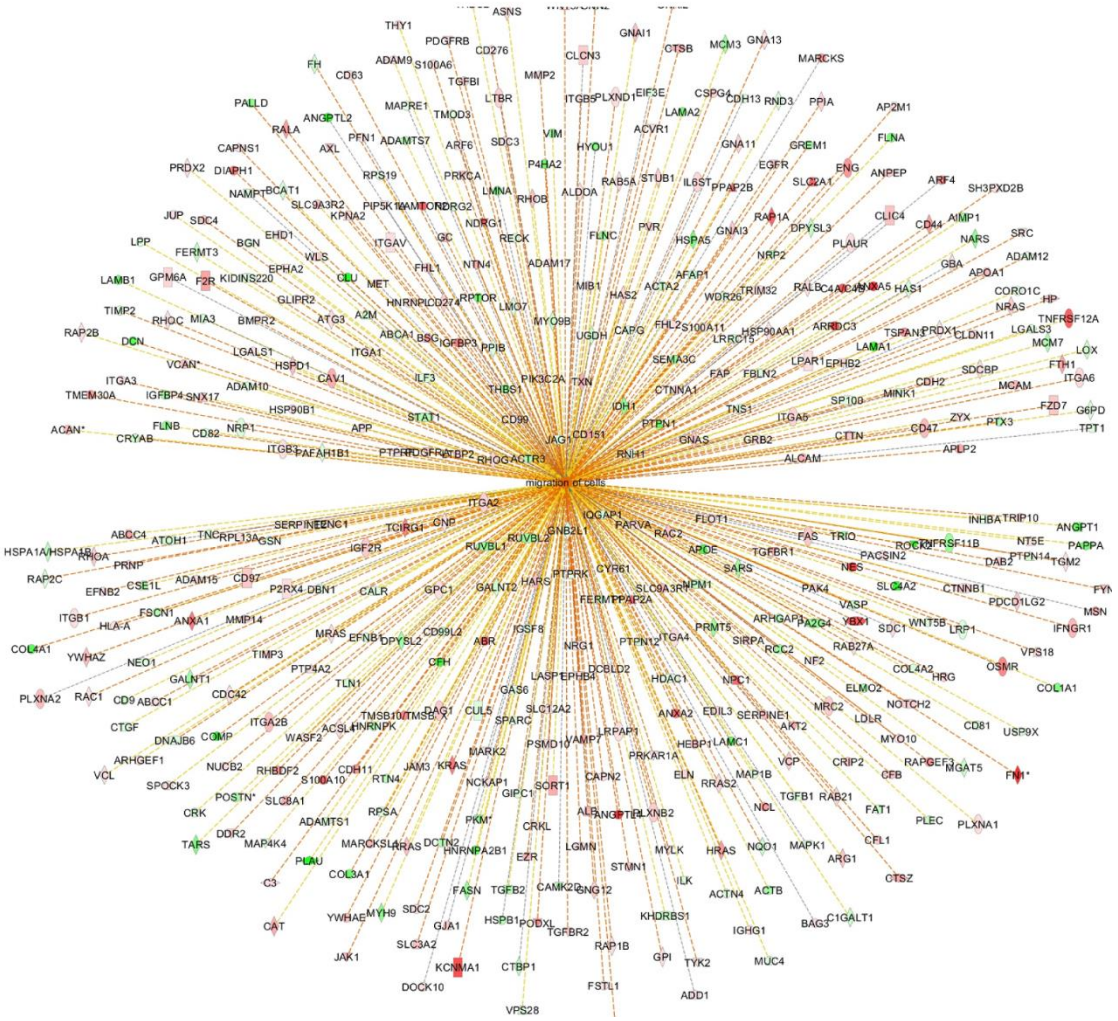

Figure S18 Predicted induction of cellular migration by MSC exosomal protein content. Ingenuity Pathway Analysis of detected MSC exosome proteins (FDR-1%) revealed presence of proteins associated with potentiation of cellular migration. Red boxes indicate increased expression, green boxes indicate decreased expression. Orange lines indicate predicted increased target functionality, blue lines indicate predicted decreased target functionality, grey lines are undetermined and yellow lines are inconsistent. Analysis of 3 different donors per condition. For differential expression T-tests with multiple testing correction with an FDR of 1% was used.

Figure S19

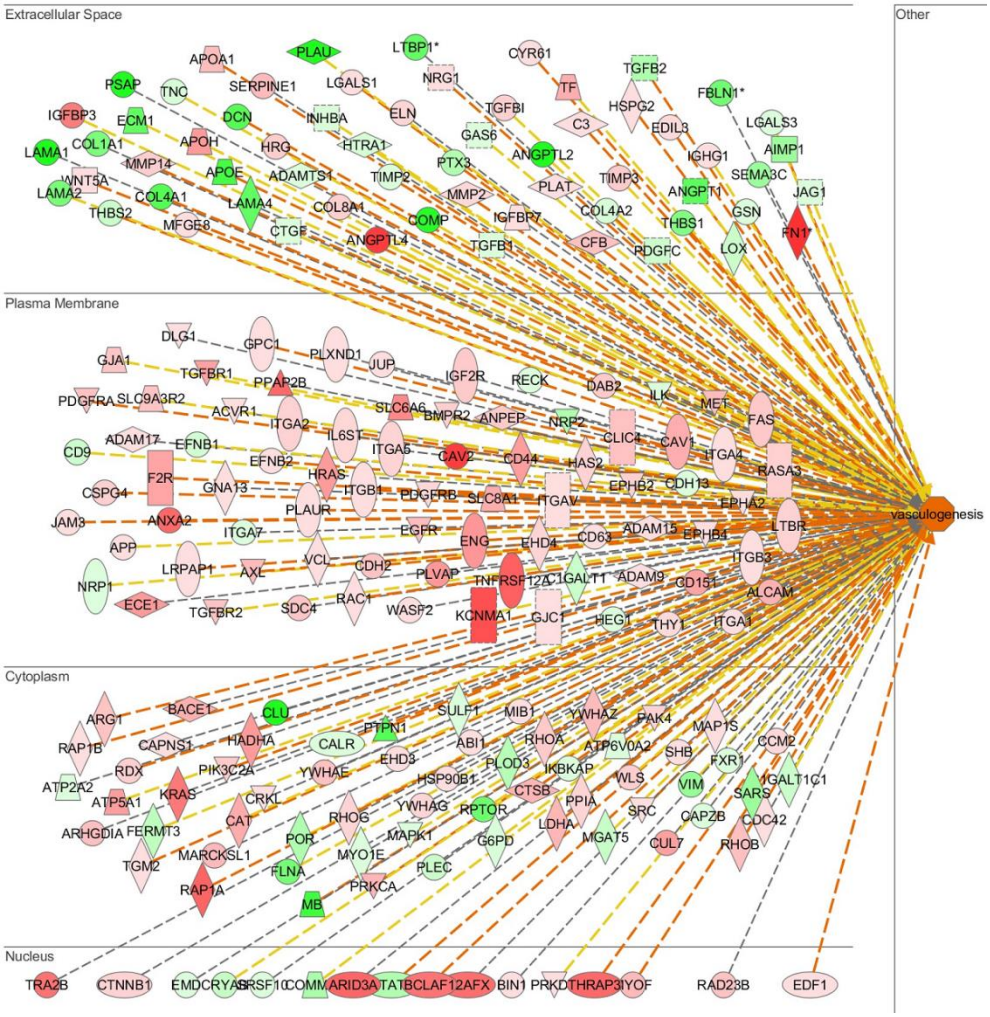

Figure S19 Predicted induction of vasculogenesis by MSC exosomal protein content. Ingenuity Pathway Analysis of detected MSC exosome proteins (FDR-1%) revealed presence of proteins associated with potentiation of vasculogenesis. Red boxes indicate increased expression, green boxes indicate decreased expression. Orange lines indicate predicted increased target functionality, blue lines indicate predicted decreased target functionality, grey lines are undetermined and yellow lines are inconsistent. Horizontal lines represent canonical subcellular localization of protein. Analysis of 3 different donors per condition. For differential expression T-tests with multiple testing correction with an FDR of 1% was used.

Figure S20

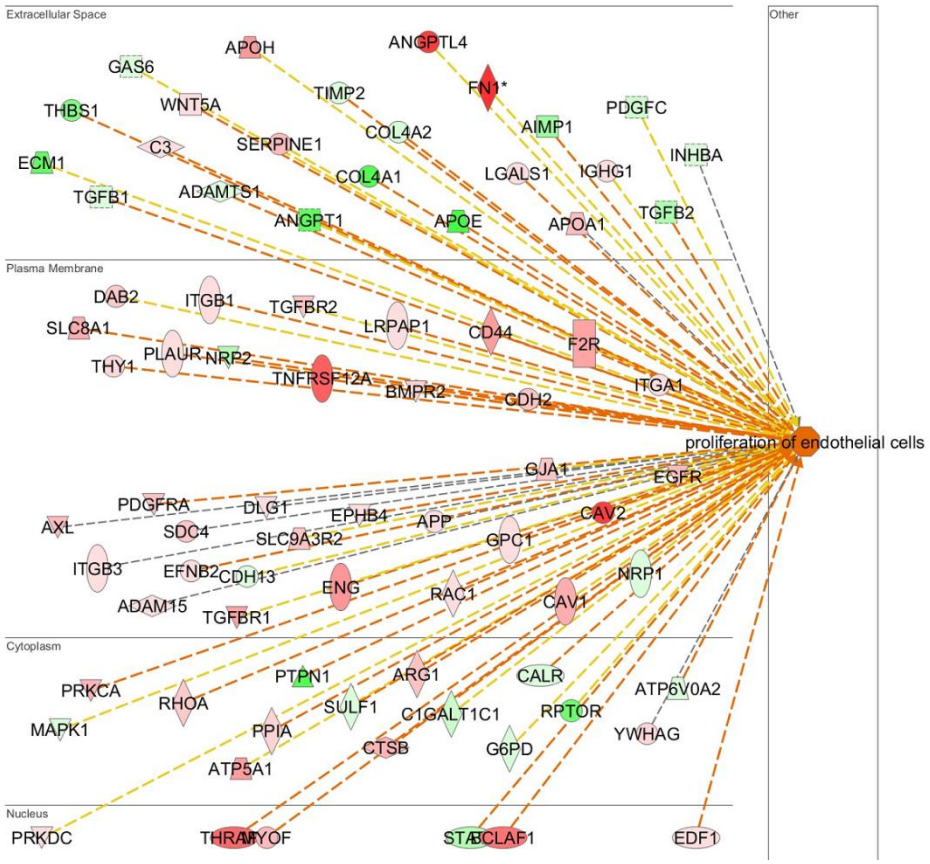

Figure S20 Predicted induction of endothelial cell proliferation by MSC exosomal protein content. Ingenuity Pathway Analysis of detected MSC exosome proteins (FDR-1%) revealed presence of proteins associated with induction of endothelial cell proliferation. Red boxes indicate increased expression, green boxes indicate decreased expression. Orange lines indicate predicted increased target functionality, blue lines indicate predicted decreased target functionality, grey lines are undetermined and yellow lines are inconsistent. Horizontal lines represent canonical subcellular localization of protein. Analysis of 3 different donors per condition. For differential expression T-tests with multiple testing correction with an FDR of 1% was used.

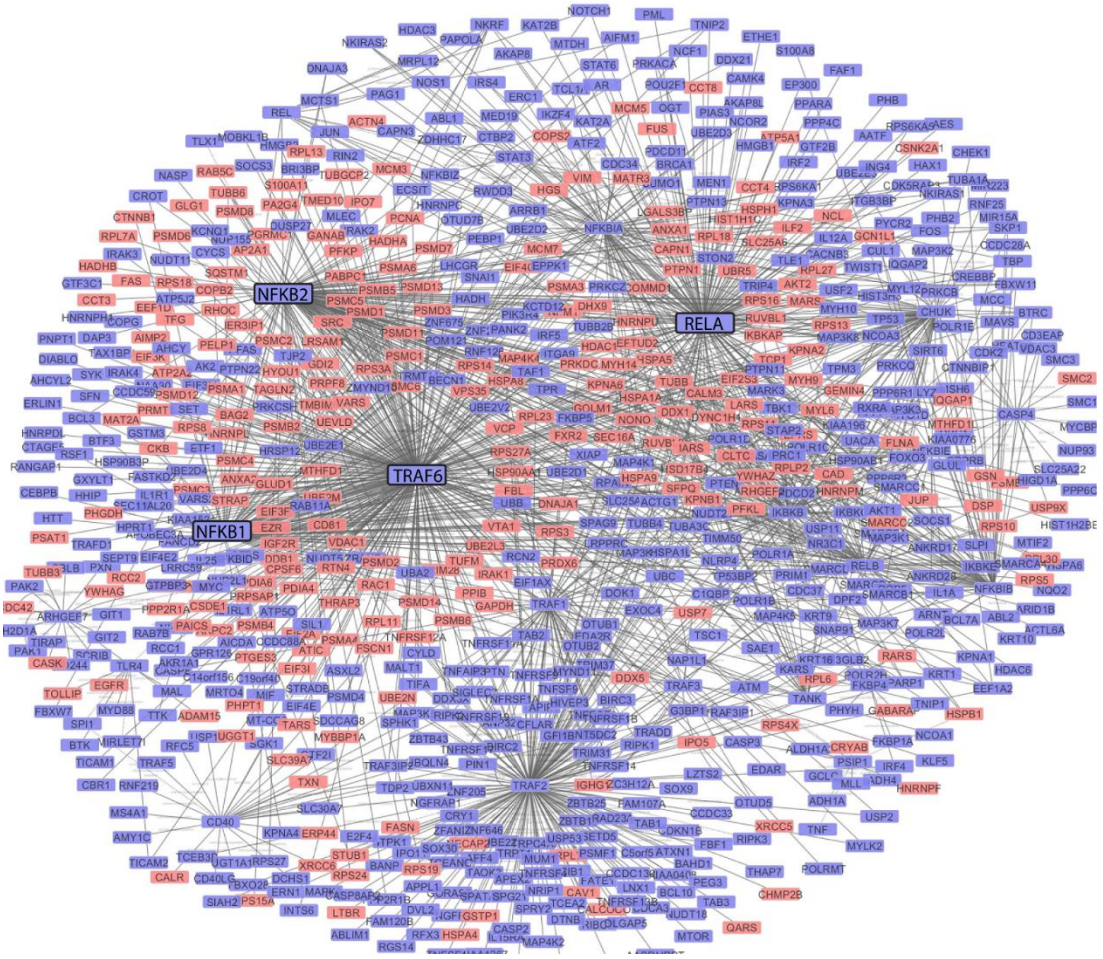

Figure S21 Network analysis of NFkB pathway interactome in MSC exosomes. Network analysis of the NFkB pathway interactome reveals the most robust clustering around NFkB1/2, RELA and TRAF6 nodes. Analysis performed using CytoScape. Red boxes indicates presence in MSC exosomes, blue boxes indicate absence of these proteins in MSC exosomes. Boxes represent NFkB pathway proteins and the proteins they physically interact with. Boxes of major clustering nodes were enlarged for clarity. Edges connecting boxes indicates experimental evidence of physical contact (eg co-immunopreciptitation, yeast-2-hybrid).